A New Stacked Two-Dimensional Spectral Iterative Technique (SIT) for Analyzing Microwave Power Deposition in Biological Media

RAPHAEL KASTNER, MEMBER, IEEE AND RAJ MITTRA, FELLOW, IEEE

Abstract—**Conventional numerical methods for analyzing power deposition in biological media have been restricted to bodies which are relatively small electrically. A new, stacked-two-dimensional-spectral-iterative-technique (SIT), presented below, does not involve the generation and inversion of a matrix and is capable of analyzing larger bodies. It is based on modeling the body by a set of planar parallel slabs and utilizing the simple (convolution-type) relationship between a current distribution on any slab and the field due to this current. This invertible relationship is conveniently formulated in the transform domain in a strictly algebraic fashion. The interactions between the various slabs are also simple and algebraic in the spectral domain. The solution is generated in an iterative manner by applying these relationships sequentially over the slabs until convergence is achieved. Discussion on convergence and numerical examples are given.**

I. INTRODUCTION

INTEREST IN HYPERTHERMIA, or electromagnetic heating of deep-seated tumors [1]–[3], and in the assessment of possible health hazards produced by EM radiation have prompted the development of analytical and numerical techniques for evaluating the electromagnetic power deposition in the interior of biological media. To date, conventional approaches to theoretical electromagnetic dosimetry [4] have involved the use of numerical matrix methods [5]–[14] for the low-frequency range. These methods are limited to the frequency region below 600 MHz. Beyond this frequency, the cost of generating, storing, and inverting a large matrix becomes prohibitively large. For the higher frequency range, analytical analysis has been used for certain separable geometries, such as planar (e.g., [15]), spherical [16], [17], cylindrical [18], and prolate spheroidal [19]. Farther on the frequency scale, the geometrical-optics approximation has been utilized [18], [20]. However, no systematic numerical approach has been available beyond the low-frequency range. The need for a method that is capable of handling, for example, the important ISM frequencies of 915 or 2450 MHz, has long been recognized.

Manuscript received September 15, 1982; revised June 15, 1983. The work reported in this paper was supported in part by the Office of Naval Research Grant N00014-81-K-0245 and, in part, by the National Science Foundation under Grant NSF ECS-8120305.

A. R. Kastner is with RAFAEL, P.O. Box 2250/87, Haifa 31021, Israel.

R. Mittra is with the Electrical Engineering Department, University of Illinois, Urbana, IL 61801.

This paper presents a new method, viz., the stacked-two-dimensional-spectral-iterative-technique (SIT), which is unrelated to the approaches mentioned above. It is based on the two-dimensional Fourier transform technique and has been applied previously to electromagnetic scattering from arbitrary, metallic, or dielectric bodies. The method takes advantage of the simplicity with which the relationship between planar sources and fields is expressed in the spectral domain. When the field is evaluated on a plane next to a thin planar current distribution lying, say, in the $x-y$ plane, the integral relating the current to the field is a convolution between the current and the Green's function. Hence, the relationship between the spectral current and the spectral field involves an algebraic multiplication of the current by the spectral Green's dyad. That is, in the spectral domain, we write

$$\underline{\tilde{E}}(k_x, k_y) = \underline{\underline{\tilde{G}}}_e \cdot \underline{\tilde{J}}(k_x, k_y). \tag{1}$$

The quantities d_x and k_y in (1) are the Fourier transform variables introduced as follows:

$$\underline{\tilde{E}}(k_x, k_y) = \int_{-\infty}^{\infty} \underline{E}(s, y, 0) e^{j(k_x x + k_y y)}\, dx\, dy. \tag{2}$$

One very efficient approach for solving the class of planar problems is the spectral-iteration technique [24]–[26] which involves no matrix inversion, and is related to Bojarski's 3-D k-space method [27] (for a detailed comparison, see [23]). This technique can be extended to include dielectric planar bodies (see Section II below). It then serves as a building block for the arbitrary scattering problem that can be formulated by modeling the current distribution by a set of parallel planar current distributions (see Fig. 1). This stacked 2-D modeling makes it possible to extend the capabilities of the spectral-domain approach to arbitrarily shaped, perfectly conducting, or (lossy) dielectric scatterers. The stacked spectral iteration technique repeatedly applies the two-dimensional Fourier transform algorithm to the set of planar distributions and generates the solution to the original three-dimensional problem in an iterative manner. A unique feature of the SIT is that it reuses the storage allocated for a single plane over and over

0018-9480/83/1100-0898$01.00 ©1983 IEEE

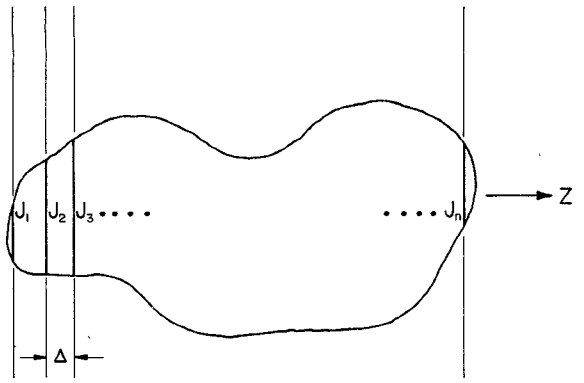

Fig. 1. Planar current samples on a two-dimensional scatterer.

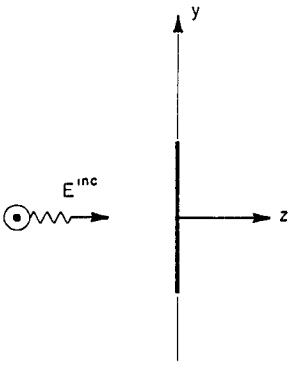

Fig. 2. The isolated plate.

again as it performs the computation at other planes. This eases the burden on storage requirements considerably.

Computational efficiency and low storage requirements make the spectral-iteration method capable of handling a rather large number of unknowns, on the order of 2000 or more, far beyond the reach of the matrix methods. This feature of the spectral technique enables one to attack moderate-to-large size scatterers, which were previously considered to be unmanageably large and beyond the scope of the moment method (matrix method) and other available techniques.

SIT thus provides an alternative to moment methods, high-frequency asymptotic techniques, and their combinations, especially in the intermediate frequency range where conventional methods are very limited in scope.

The extension of the procedure developed for planar conducting [24] to planar dielectric structures is discussed in Section II. This forms the building block for the SIT for arbitrary dielectric bodies, given in Section III. Results are described in Section IV.

II. The Building Block for SIT: The Single Plate

The SIT for general scatterers may be viewed as a generalization of the two-dimensional scheme [24] for the single thin plate. (See Fig. 2.) This scheme is now reformulated to accommodate dielectric thin planar slabs as well. To this end, we use the polarization current

$$\underline{J} = j\omega\varepsilon_0(\varepsilon_r - 1)(\underline{E} + \underline{E}^{\text{inc}}) \tag{3}$$

as the current source for the free-space wave equation.

Equation (3) serves as the "constitutive relationship" which plays an analogous role to the boundary condition in the conducting case. Equation (3) is algebraic in the spatial domain, whereas (1) is algebraic in the spectral domain. An iterative procedure for solving this system of equations alternates between the two domains by use of the FFT algorithm. It is depicted graphically in Fig. 3 and in the following step-by-step outline.

1) Begin with an initial guess $\underline{J}^{(0)}$

2) Take the 2-D Fourier transform of $\underline{J}^{(0)}$ on the planar structure to obtain $\tilde{\underline{J}}^{(0)}$.

3) Multiply $\tilde{\underline{J}}^{(0)}$ by $\tilde{\underline{\underline{G}}}_e$.

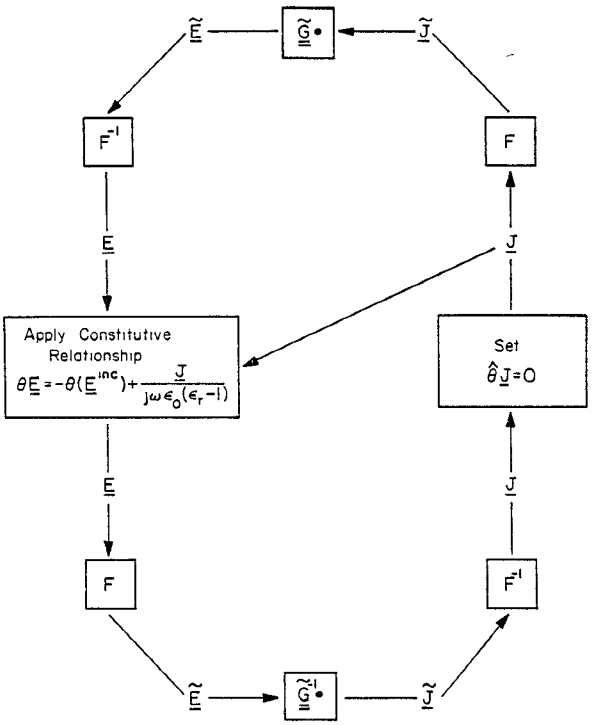

Fig. 3. The two-dimensional iterative scheme for a dielectric planar scatterer.

4) Evaluate $\underline{E}^{(0)} = F^{-1}[\tilde{\underline{\underline{G}}}_e \cdot \tilde{\underline{J}}^{(0)}]$, the approximation to the scattered electric field $\underline{E}$. The accuracy of the solution can be conveniently checked at this point by verifying the satisfaction of the constitutive relationship (3) within the scatterer. This is an important feature of the method.

5) Update $\underline{E}$ by applying the following constitutive relationship: Replace $\underline{E}_t$ within the body, $\theta\underline{E}_t$ (θ = truncation operator; it is defined by $\theta = 1$ on scatterer and $\theta = 0$ outside scatterer) by $\theta(-\underline{E}_t^i) + \underline{J}/j\omega\varepsilon_0(\varepsilon_r - 1)$, leaving the field outside the body unchanged.

6) Take the Fourier transform of the updated field obtained in Step 5.

7) Multiply the result obtained in Step 6 by $\tilde{\underline{\underline{G}}}_e^{-1}$. The result thus obtained is $\tilde{\underline{J}}^{(1)}$, which is the transform of the first iteration of the current.

8) Take the inverse Fourier transform of $\tilde{\underline{J}}^{(1)}$ obtained in Step 7 to get the surface current on the body. In other words, perform the operation $\theta(\mathcal{F}^{-1}[\tilde{\underline{J}}^{(1)}])$. For an exact

solution, the truncation is redundant, since $\underline{J} = \theta \underline{J}$, and, hence, $\theta(\mathcal{F}^{-1}[\mathcal{F}[\theta \underline{J}]]) = \theta\theta \underline{J} = \underline{J}$. However, the Fourier inversion of an n^{th} approximate solution $\underline{\tilde{J}}^{(n)}$ will not give rise to a current distribution that is nonzero, except on the body. This step provides a test for the accuracy and for the convergence of the approximate solution by comparing the approximate $\underline{J}^{(0)}$ with $\theta(\mathcal{F}^{-1}[\underline{\tilde{J}}^{(1)}])$.

9) Repeat as necessary using the improved $\underline{J}^{(1)}$ obtained from Step 8 into Step 1 to generate the next higher order approximation $\underline{J}^{(2)}$ and continue in this manner until convergence has been attained.

The 2-D spectral dyadic Green's function, $\underline{\underline{\tilde{G}}}_e$, mentioned in steps 3 and 7 above, is defined by

$$\begin{pmatrix} \tilde{E}_x \\ \tilde{E}_y \end{pmatrix} = \underline{\underline{\tilde{G}}}_e \begin{pmatrix} \tilde{J}_x \\ \tilde{J}_y \end{pmatrix} \tag{4}$$

since, for the isolated plate, only the transversal current components J_x and J_y are present. It is given by

$$\underline{\underline{\tilde{G}}}_e = j\omega\mu \frac{j}{2\sqrt{k_0^2 - k_t^2}} \begin{pmatrix} 1 - \left(\frac{k_x}{k_0}\right)^2 & -\frac{k_x k_y}{k_0^2} \\ -\frac{k_x k_y}{k_0^2} & 1 - \left(\frac{k_y}{k_0}\right)^2 \end{pmatrix} \tag{5}$$

where

$$k_t^2 = k_x^2 + k_y^2. \tag{6}$$

In practice, the question of selecting an appropriate sampling rate should be addressed. It has been found (see [21]) that a low sampling rate results in loss of high-order mode information, and hence in smoothing of sharp variations. If such localized errors can be tolerated, a low sampling rate of $\lambda/4$ to $\lambda/2$ (in the medium) may be employed in order to bring the total number of samples to manageable levels.

This scheme is extended in the next section to three-dimensional bodies, while retaining the two-dimensional processing for the sake of computational economy and versatility.

III. Arbitrary (Lossy) Dielectric Bodies

The approach to handling the general-shaped body is to sample the induced current on it by a collection of n planar distributions in free space, as shown in Fig. 1. The single-plane scheme of Section II can be used to solve the original problem which is now reduced to that of determining the two-dimensional currents on n planar surfaces, separated by a distance Δ.

The strategy for attacking the reduced problem is as follows. We employ the basic iterative scheme outlined in Section II for planar structures to update the individual planar distributions in a sequential manner, starting with the first plane and ending up at the last one. We update the currents in one particular plane by applying a single iteration cycle as in Fig. 3, while regarding the distributions in the other planes as temporarily known from previous operations. This sequential processing facilitates the reuse of the same storage area for all the linear currents. This significantly reduces the burden on the computer memory and cost as compared to the direct solution of a three-dimensional problem carried out in one fell swoop. The iteration process encompassing all the planes is repeated as many times as necessary until convergence of the entire current distribution is achieved.

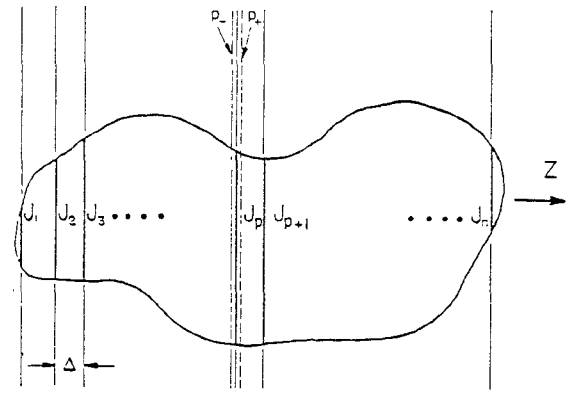

Fig. 4. Sliced scatterer with the planes p_- and p_+ shown immediately to the left and right of J_p, respectively.

The enforcement of the constitutive relationship (3) within the body requires the computation of the scattered field produced by all of the planar-induced current distributions. This is done as follows.

Assume that the plane at which the scattered field is being evaluated is p_+, immediately to the right of the current slice J_p (Fig. 4). It is evident that the sources J_1 through J_p lie to the left of this plane, while J_{p+1} through J_n are on the right of p_+. Consider first the left sources, the fields from which propagate to the right $(+z)$ direction; hence, their spectrum has the z-dependence $\exp[-jz\sqrt{k_0^2 - k_t^2}]$. Let us denote this part of the field by $E_{p_+}^{(-)}$ where the superscript indicates that the currents generating this field are on the left of the plane of evaluation

$$\underline{\tilde{E}}_{p_+}^{(-)} = \underline{\underline{\tilde{G}}}_e \cdot \Delta \sum_{i=1}^{p} \underline{\tilde{J}}_i e^{-j\sqrt{k_0^2 - k_t^2}\cdot(p-i)\Delta} \tag{7}$$

where $\underline{\underline{\tilde{G}}}_e$ has been defined in (4) and (5).

Similarly $E_{p_+}^{(+)}$, the aggregate of fields radiated by the sources on the right of the plane p_+, may be written in the transform domain as

$$\underline{\tilde{E}}_{p_+}^{(+)} = \underline{\underline{\tilde{G}}}_e \cdot \Delta \sum_{i=p+1}^{n} \underline{\tilde{J}}_i e^{j\sqrt{k_0^2 - k_t^2}(p-i)\Delta}. \tag{8}$$

The total transformed field at the plane p_+ is then a superposition of $E_{p_+}^{(-)}$ and $E_{p_+}^{(+)}$.

The separate bookkeeping of the two components $E^{(-)}$ and $E^{(+)}$ is necessary to facilitate transformation of the field between planes so that the sequential processing can be done. Suppose, for example, that the field at the plane $(p+1)_-$ is desired. Since the region between the planes p_+ and $p+1_-$ is free space, the following equations are valid:

$$\underline{\tilde{E}}_{(p+1)_-}^{(-)} = \underline{\tilde{E}}_{p_+}^{(-)} e^{-j\sqrt{k_0^2 - k_t^2}\Delta} \tag{9a}$$

$$\underline{\tilde{E}}_{(p+1)_-}^{(+)} = \underline{\tilde{E}}_{p_+}^{(+)} e^{+j\sqrt{k_0^2 - k_t^2}\Delta}. \tag{9b}$$

Next, in order to transform the field from the plane $(p+1)_-$ to $(p+1)_+$, we note that these two adjacent planes are located on each side of the thin current distribution J_{p+1}. Consequently, we subtract the contribution of J_p from $E^{(-)}$ and add this contribution to $E^{(+)}$. This gives

$$\underline{\tilde{E}}^{(-)}_{(p+1)_+} = \underline{\tilde{E}}^{(-)}_{(p+1)_-} + \underline{\underline{\tilde{G}}}_e \cdot \underline{\tilde{J}}_{(p+1)} \Delta \tag{10a}$$

$$\underline{\tilde{E}}^{(+)}_{(p+1)_+} = \underline{\tilde{E}}^{(+)}_{(p+1)_-} - \underline{\underline{\tilde{G}}}_e \cdot \underline{\tilde{J}}_{(p+1)} \Delta. \tag{10b}$$

The above equations are consistent with the requirement that the total field be continuous across the plane.

A typical updating cycle at the plane p is done similarly to that for the single-plate case, by computing the total scattered field by the superposition of $E^{(-)}$ and $E^{(+)}$. One can now take the inverse transform of this scattered field due to the induced sources and enforce the constitutive relationship which may be expressed as

$$\underline{E}^{(-)}_{p_+} + \underline{E}^{(+)}_{p_+} = -\underline{E}_{\text{inc}} + \frac{\underline{J}(x, y)}{j\omega\varepsilon_0 [\varepsilon_r(x, y) - 1]}. \tag{11}$$

We replace the scattered field values inside the body with those dictated by the constitutive relationship while leaving the scattered field outside the body unchanged. A Fourier transform of the updated total field is then taken. We then note that $\underline{\tilde{E}}^{(+)}_{p_+}$ is the field produced by currents located to the right of p_+. These currents are assumed to be temporarily known, hence, $\underline{\tilde{E}}^{(+)}_{p_+}$ is not changed during this cycle. $\underline{\tilde{E}}^{(-)}_{p_+}$, on the other hand, depends on $\underline{J}_1$ through $\underline{J}_p$ and is updated. This is accomplished as follows:

$$\underline{\tilde{E}}^{(-)}_{p_+} = \underline{\tilde{E}}_{p_+} - \underline{\tilde{E}}^{(+)}_{p_+}. \tag{12}$$

The current $\underline{J}_p$ itself is next updated using a relationship analogous to Step 7 in the single plate case above

$$\underline{\tilde{J}}_p = \underline{\underline{\tilde{G}}}_e^{-1} \cdot \left(\underline{\tilde{E}}^{(-)}_{p_+} - \underline{\tilde{E}}^{(-)}_{p_-} \right) \Delta^{-1}. \tag{13}$$

$\underline{\tilde{E}}^{(-)}_{p_-}$ in the above equation is the contribution of the currents $\underline{J}_1$ through $\underline{J}_{p-1}$ which are also assumed to be temporarily known from the previous cycle.

The process of updating the current on plane p is now complete. We transform the updated field to plane $p+1$ by using (9a) and (10a), and repeat the entire process for that plane. We then continue in this manner until the entire body has been scanned once. This constitutes one iteration step. The entire scanning process is then repeated until convergence is achieved and the results of the constitutive relationship test have been found to be satisfactory.

IV. Convergence Enhancement

Numerical experiments with the procedure described above indicate that convergence is affected by the size of the body, or by the total number of sampling points. Convergence becomes difficult when the number is of the order of one thousand or more. However, it is possible to improve the convergence, even for the otherwise divergent cases, which can often be made to converge by using certain iteration algorithms. This point is further elaborated on below.

A. A Good Initial Guess

Many problems may be solved with an initial guess of zero currents within the body. However, convergence can be considerably enhanced if a good approximation for the current is used instead. Such an approximation may be derived by noting that the high losses in the living tissues make them appear somewhat similar to conducting media. A physical optics approximation can then be written down, i.e., $\underline{J}^{(0)} = 2\underline{n} \times \underline{H}^{\text{inc}}$ on the illuminated faces of the body, and $\underline{J} = 0$ elsewhere. Such an approximation has proven to be a good starting point for the iterative procedure. Any additional information derived, say, from ray optics, may be useful. However, once the convergence rate becomes reasonable, the price of a few more iterations may not be too large compared to the effort involved in developing a more elaborate initial guess.

B. Relaxation Factor

It has been found that often the values of currents and fields tend to oscillate about the final value, and sometimes even diverge after a number of iterations. A remedy for smoothing the oscillations is to average the new, updated value of the current with the previous approximation. A relaxation factor α is defined as the amount by which the new current is weighted, relative to the previous one. That is, rather than using $\underline{J}^{(n)}$, one takes $\alpha\underline{J}^{(n)} + (1-\alpha)\underline{J}^{(n-1)}$ as the updated version of the current. Relaxation factors of as low as 20 percent or, sometimes, 10 percent may be needed.

C. Modified Scanning

The procedure described in the preceding section involves the updating of planar currents in a sequential manner, where a single updating cycle is performed for each plane in turn. This method of scanning the planes may be modified so that repeated updating of a single plane, or of a group of adjacent planes, may ease convergence problems. This is due to the fact that the inaccuracies in the iterated current values tend to generate large amounts of noise as the fields are propagated over many planes and when many high-order harmonics are used. This is especially significant for the back planes, where the fields are usually low, owing to the high attenuation in the lossy tissue. The contribution of these planes may become unproportionally large, as may be manifested by a very distorted $E^{(-)}$ at the front planes. Hence, keeping the values of $E^{(-)}$ temporarily constant while the front planes are being processed may slow down the noise-generating mechanism.

D. Scaling Factor

It has been found that often the main difference between the approximate current derived after a few iterations and the exact solution is a complex factor. One can partly compensate for this difference by multiplying the current at the plane p at every iteration by the variational factor X,

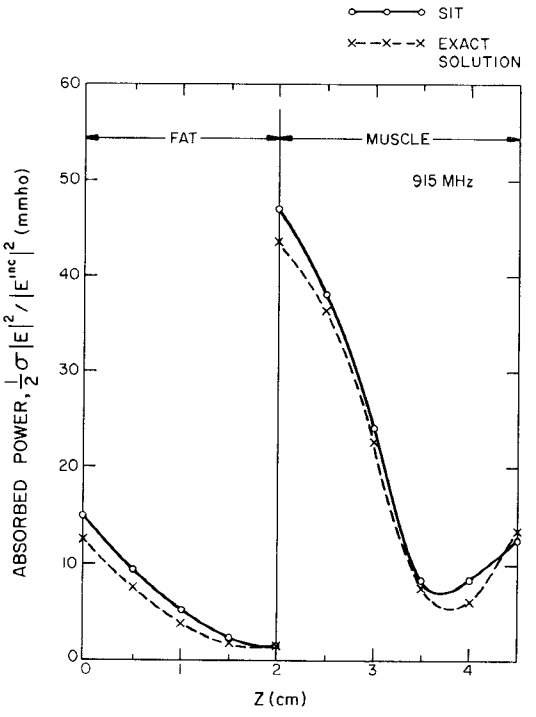

Fig. 5a. Comparison of SIT results with the exact solution for a layered tissue structure at 915 MHz.

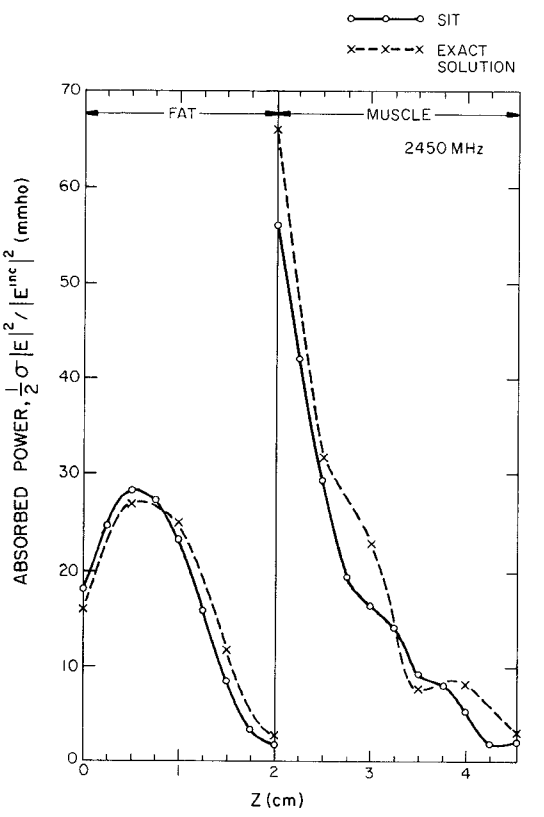

Fig. 5b. Comparison of SIT results with the exact solution for a layered tissue structure at 2450 MHz.

where

$$X = \frac{\langle \underline{J}_p^{(n)}, \underline{F} \rangle}{\langle \underline{J}_p^{(n)}, L\underline{J}_p^{(n)} \rangle} \tag{14}$$

and $\underline{F}$ is the total incident field on plane p

$$\underline{F} = \underline{E}_{p^-}^{(-)} + \underline{E}_{p^+}^{(+)} + \underline{E}^{\text{inc}}. \tag{15}$$

L is the operator defined so that (1) and (3) can be integrated into the form $L\underline{J} = \underline{F}$

$$L\underline{J} = \frac{J}{j\omega\varepsilon_0(\varepsilon_r - 1)} + \underline{\underline{g}}_e * \underline{J}. \tag{16}$$

The scaling factor X is defined in a similar fashion to the one used in [25] and [26], except here the incident field on the plane, $\underline{F}$, is not completely known as before, but rather assumed temporarily known, being the outcome of both the incident field and the currents on other planes which are assumed known as long as plane p is being processed. The scaling factor has proved very useful in improving convergence in difficult cases.

V. Results

A. Layered Medium

The simple case of two infinite planar layers, one of which is constituted of fat and the other of muscle, has been used for an initial check on the capabilities of the SIT. For this case, the solution is known. Figs. 5(a) and (b) show the results for the ISM frequencies of 915 and 2450 MHz, respectively, compared to an exact solution derived by plane-wave multiple reflection analysis. The electrical properties of fat and muscle at the relevant frequencies have been taken from [28]. It should be emphasized that the SIT scheme treats the structure from a general point of view and does not take advantage of this specific shape. Note that the field in the muscle layer is much weaker than the one in the fat. The small inaccuracies in the field values within the muscle become more pronounced as the power is computed, owing to the much larger conductivity in the muscle.

B. Cylindrical Structures

When the structure lacks variation in one transversal direction, e.g., $\partial/\partial x \equiv 0$, i.e., $k_x \equiv 0$, and the incident electric field is polarized along that direction, the problem reduces to a scalar one where E_x or J_x are related by the scalar Green's function

$$\tilde{G}_e = j\omega\mu \frac{i}{2\sqrt{k_0^2 - k_y^2}}. \tag{17}$$

In analogy to the three-dimensional case, the two-dimensional problem is now analyzed by a stack of one-dimensional distributions on the cylindrical cross section. This formulation is considerably more economical than the three-dimensional one; hence, it may be useful for structures that are long and approximately uniform, particularly in regions away from the edges.

The generality and versatility of the SIT is demonstrated by the problem treated in Fig. 6, where a cylinder consisting of muscle is subjected to plane-wave illumination. An equivalent solution by matrix method would have required an inversion of a matrix of about 600×600.

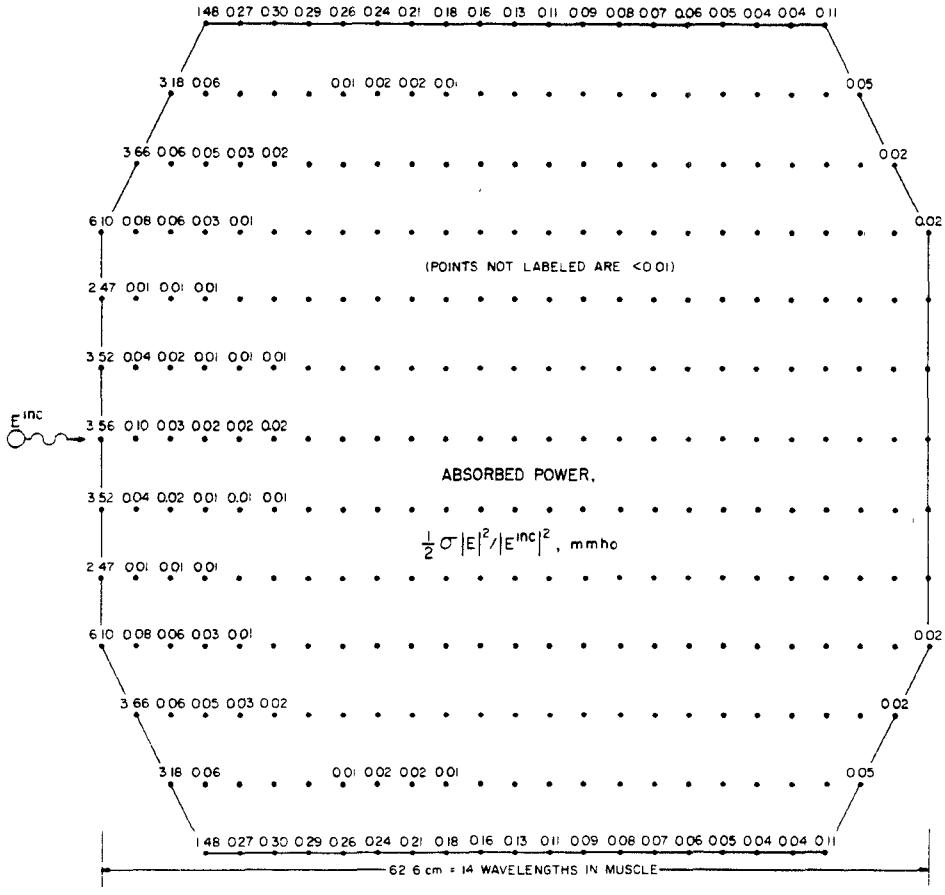

Fig. 6. Power deposition in a cross section of a cylindrical muscle structure with dimensions 62.6 cm × 62.6 cm at 915 MHz. The incident electric field is x-polarized.

C. Three-Dimensional Case

Finally, a complete 3-D structure has been analyzed, as shown in Fig. 7, where a thin-muscle box, modeled by two planes, is illuminated by an x-polarized plane wave propagating perpendicularly to the planes. Since for any given incident field all three components of the current may be present, the problem is even more complicated. In order to simplify the solution, cross-polarization effects have been neglected, i.e., for an incident field polarized along the x-direction, the only current component assumed to be present is J_x. The scalar Green's function is the $\tilde{G}_{e_{11}}$ of (5).

A similar structure was analyzed by Guru and Chen [29]. One may compare the $x = 0$ line in [29, Figs. 7–11]. An overall similar behavior is seen, including a dip of about -4 dB toward the edge at plane 1. However, since we use a somewhat smaller number of samples to analyze a square of an area three times electrically larger, the smoothing effect described in Section II manifests itself by the absence of the singular behavior at the edge itself. The omission of the cross-polarized components, on the other hand, seems to have little effect on the results.

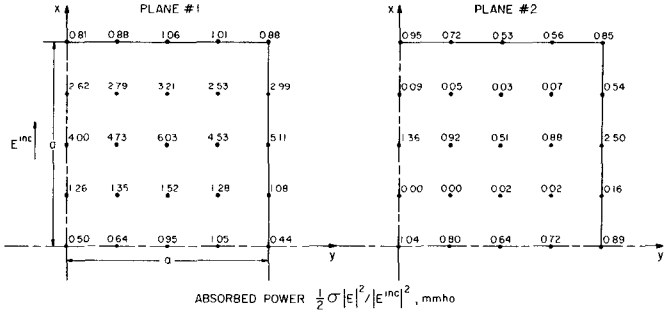

Fig. 7 Power deposition in a muscle box, modeled by two planes with dimensions $2a \times 2a$, spaced $0.125a$ apart (one quadrant of each plane is shown). $f = 915$ MHz, $a = 31.3$ cm.

VI. Conclusions

The data-handling capability of SIT well exceeds that of the matrix methods. This advantage is mostly useful in the much-needed intermediate frequency range, including the ISM frequencies 915 and 2450 MHz. Higher frequencies may not be handled efficiently by SIT owing to convergence problems. Experience with the conducting scatterer has also strongly indicated the usefulness of SIT for the intermediate frequency range. The method is expected to be developed further and to find new applications (see also [23]).

References

[1] D. A. Christensen and C. H. Durney, "Hyperthermia production for cancer therapy: A review of fundamentals and methods," *J. of Microwave Power*, vol. 16, no. 2, pp. 89–105, 1981.

[2] R. S. Elliott, W. H. Harrison, and F. K. Storm, "Hyperthermia:

Electromagnetic heating of deep-seated tumors," *IEEE Trans. Biomed. Eng.*, vol. CME-29, no. 1, pp. 61–64, Jan. 1982.
[3] A. W. Guy, J. F. Lehman, and J. B. Stonebridge, "Therapeutic applications of electromagnetic power," *Proc. IEEE*, vol. 62, pp. 55–75, Jan. 1974.
[4] C. H. Durney, "Electromagnetic dosimetry for models of humans and animals: A review of theoretical and numerical techniques," *Proc. IEEE*, vol. 68, pp. 33–39, Jan. 1980.
[5] D. E. Livesay and K. Chen, "Electromagnetic fields induced inside arbitrary shaped biological bodies," *IEEE Trans. Microwave Theory Tech.*, vol. MTT-22, Part II, pp. 1273–1280, 1974.
[6] K. M. Chen and B. S. Guru, "Internal EM field and absorbed power density in human torsos induced by 1-500 MHz EM waves," *IEEE Trans. Microwave Theory Tech.*, vol. MTT-25, pp. 746–755, 1977.
[7] _____, "Induced EM fields inside human bodies irradiated by EM waves of up to 500 MHz," *J. Microwave Power*, vol. 12, pp. 173–183, 1977.
[8] M. J. Hagmann, OM. P. Gandhi, and C. H. Durney, "Numerical calculation of electromagnetic energy deposition for a dielectric model of man," *IEEE Trans. Microwave Theory Tech.*, vol. MTT-27, pp. 804–809, Sept. 1979.
[9] P. W. Barber, "Resonance electromagnetic absorption by nonspherical dielectric objects," *IEEE Trans. Microwave Theory Tech.*, vol. MTT-25, pp. 373–381, 1977.
[10] _____, "Electromagnetic power deposition in prolate spheroid models of man and animals at resonance," *IEEE Trans. Biomed. Eng.*, vol. BME-24, pp. 513–521, 1977.
[11] S. Rukspollmuang and K. M. Chen, "Heating of spherical versus realistic models of human and intrahuman heads by electromagnetic waves," *Radio Sci.*, vol. 14, no. 6S, pp. 51–62, Nov.–Dec. 1979.
[12] I. Chatterjee, J. J. Hagmann, and OM. P. Gandhi, "Electromagnetic-energy deposition in an inhomogeneous block model of man for near-field irradiation conditions," *IEEE Trans. Microwave Theory Tech.*, vol. MTT-28, pp. 1452–1459, Dec. 1980.
[13] M. J. Hagmann, I. Chatterjee, and OM. P. Gandhi, "Dependence of electromagnetic energy deposition upon angle of incidence for an inhomogeneous block model of man under plane-wave irradiation," *IEEE Trans. Microwave Theory Tech.*, vol. MTT-29, pp. 252–255, Mar. 1981.
[14] D. H. Schaubert, D. R. Wilton, and A. W. Glisson, "Computation of fields inside lossy, inhomogeneous, dielectric bodies," in *Nat. Radio Sci. Meet. Dig.*, (Albuquerque, NM), May 24–28, 1982, pp. 62.
[15] I. Chatterjee, M. J. Hagmann, and OM. P. Gandhi, "Electromagnetic absorption in a multilayered slab model of tissue under near-field exposure conditions," *Bioelectromag.*, vol. 1, pp. 379–388, 1980.
[16] C. M. Weil, "Absorption characteristics of multilayered sphere models exposed to UHF/microwave radiation," *IEEE Trans. Biomed. Eng.*, vol. BME-22, pp. 468–476, 1975.
[17] H. N. Kritikos and H. P. Schwan, "The distribution of heating potential inside lossy spheres," *IEEE Trans. Biomed. Eng.*, vol. BME-22, pp. 457–463, 1975.
[18] H. Massoudi, C. H. Durney, and C. C. Johnson, "Geometrical-optics and exact solutions for internal fields and SARs in a cylindrical model of a man as irradiated by an electromagnetic plane wave," *Radio Sci.*, vol. 14, no. 6S, pp. 35–42, Nov.–Dec. 1979.
[19] A. Lakhtakia, M. F. Iskander, C. H. Durney, and H. Massoudi, "Near-field absorption in prolate spheroidal models of humans exposed to a small loop antenna of arbitrary orientation," *IEEE Trans. Microwave Theory Tech.*, vol. MTT-29, pp. 588–594, June 1981.
[20] G. I. Rowlandson and P. W. Barber, "Absorption of higher-frequency RF energy by biological models: calculations based on geometrical optics," *Radio Sci.*, vol. 14, no. 6S, pp. 43–50, Nov.–Dec. 1979.
[21] R. Kastner and R. Mittra, "A spectral-iteration technique for analyzing scattering from arbitrary bodies," in *1981 IEEE AP-S Int. Symp. Dig.* (Los Angeles, CA), June 16–19, 1981, pp. 312–314.
[22] R. Kastner and R. Mittra, "Application of the stacked 2-D spectral-iteration technique (SIT) to perfectly conducting cylinders with H-mode excitation and to dielectric cylinders," *1982 IEEE AP-S Int. Symp. Dig.* (Albuquerque, NM), May 24–28, 1982, pp. 499–502.
[23] _____, "A comparative study of the stacked 2-D spectral iterative technique, the moment method, asymptotic techniques and the Bojarski's 3-D k-space method," in *1982 IEEE AP-S Int. Symp. Dig.* (Albuquerque, NM), May 24–28, 1982, pp. 503–506.
[24] W. L. Ko and R. Mittra, "A new approach based on a combination of integral equation and asymptotic techniques for solving electromagnetic scattering problems," *IEEE Trans. Antennas Propagat.*, vol. AP-25, pp. 187–197, Mar. 1977.
[25] C. H. Tsao and R. Mittra, "A spectral-iteration approach for analyzing scattering from frequency selective surfaces," *IEEE Trans. Antennas Propagat.*, vol. AP-30, pp. 303–308, Mar. 1982.
[26] R. Kastner and R. Mittra, "A spectral-iteration approach for analyzing a corrugated-surface twist polarizer for scanning reflector antennas," *IEEE Trans. Antennas Propagat.*, vol. AP-30, pp. 673–676, July 1982.
[27] N. N. Bojarski, "K-space formulation of the electromagnetic scattering problem," Technical Rep. AFAL-TR-71–75, Mar. 1971.
[28] C. C. Johnson and A. W. Guy, "Nonionizing electromagnetic wave effects in biological materials and systems," *Proc. IEEE*, vol. 60, pp. 692–718, June 1972.
[29] B. S. Guru and K.-M. Chen, "Experimental and theoretical studies on electromagnetic fields induced inside finite biological bodies," *IEEE Trans. Microwave Theory Tech.*, vol. MTT-24, pp. 433–440, July 1976.

Raphael Kastner (S'80–M'82) was born in Haifa, Israel on November 21, 1948. He received the B.S. and M.S. degrees in electrical engineering from the Technion, Israel Institute of Technology, in 1973 and 1976, respectively, and the Ph.D. degree from the University of Illinois, Urbana, in 1982.

From 1976 to 1979, he was with RAFAEL, Israel, where he was engaged in research and development of antenna arrays. He then joined the Electromagnetics Laboratory of the University of Illinois, first as a research assistant and later on as a visiting research associate, and worked with Prof. R. Mittra on spectral-domain techniques. He returned to RAFAEL in 1982, where he is currently heading an antenna group. His interest areas are numerical methods in scattering and antennas, EM theory, millimeter-wave antennas, and inverse scattering.

Dr. Kastner is a member of Tau Beta Pi and Eta Kappa Nu.

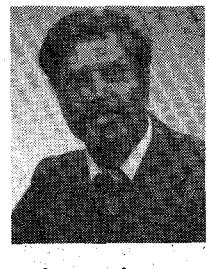

Raj Mittra (S'54–M'57–SM'69–F'71) is a Professor of Electrical Engineering and the Head of the Electromagnetic Radiation and Scattering Group of the Coordinated Science Laboratory at the University of Illinois in Urbana. He serves as a consultant to several industrial and governmental organizations in the United States and abroad. His professional interests include the areas of analytical and computer-aided electromagnetics, satellite antennas, microwave and millimeter-wave integrated circuits, frequency selective surfaces, radar scattering, interaction of electromagnetic waves with biological media, etc. He is a Past-President of the Antennas and Propagation Society.